Plasma generation within gas bubbles using a Plasma Gun

A. Hamon, C. Douat, S. Dozias, J-M. Pouvesle and E. Robert

GREMI UMR 7344, CNRS/ Université d'Orléans, 45067 Orléans Cedex 2, France

Abstract: Plasma interactions with liquids has drawn much attention over the past few years considering the interest of water treatment. In this context, we studied the potential of low temperature plasmas created inside bubbles using a Plasma Gun (PG) from which the capillary exit is immersed into water. Plasma generation inside neon bubbles, as well as bubble growth modifications were evidenced through time-resolved ICCD imaging. Results clearly show that the plasma propagation inside the bubbles is strongly dependent on the liquid conductivity and the bubbles behaviour depends on the discharge delivery conditions.

Keywords: Plasma-liquid interactions, non-thermal plasma, plasma in bubbles, plasma jet, Plasma Gun

1. Introduction

Plasma/liquid interactions are mainly investigated to study the production of reactive species, such as hydrogen peroxide, hydroxyl radicals and oxygen radicals, useful for environmental and biomedical applications [1]. Development of such applications requires a better understanding of in-liquid discharge phenomena, due to the treated liquid impact on the plasma delivery. Only few studies have been dedicated to the direct production of atmospheric pressure plasma in bubbles generated in a liquid (e.g. [2, 3, 4]). In this work, we studied plasmas created inside bubbles using a Plasma Gun (PG) from which the capillary exit is immersed in water. ICCD camera was used to observe the plasma propagation and the bubble evolution. Conductivity and chemical measurements were also performed. The experimental setup used is described in section 2. Results and discussion are presented in section 3, followed by a general conclusion in section 4.

2. Experimental setup

The Plasma Gun (PG) used in this work, was similar to the one used by Robert *et al* [5]. The device was powered by microsecond-duration voltage pulses of 14 kV with a repetition frequency at 2 kHz. In this experiment, pure neon (N40) has been used, while neon is rarely used in plasma jet. We used it for its more intense light emission than helium, useful for imaging experiment. It was flowing through the device in the range from 12 sccm to 100 sccm. As shown in Fig. 1, the tip of the PG capillary was immersed to a depth of 1 cm into a quartz tank filled with 3 ml of liquid. Due to the gas flow, bubbles are created at the tip of the PG. ICCD camera equipped with a 105 mm lens was used to observe the bubble dynamics at the PG tip and to characterize plasma generation in the bubbles. The conductivity measurements were performed with the SevenCompact Duo S213 conductimeter from Mettler Toledo. For the chemical analysis, we used quantitative test strips for hydrogen peroxide, nitrites and nitrates from Quantofix.

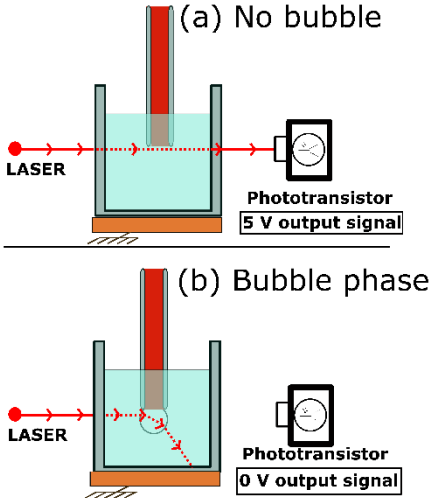

Fig. 1 Experimental scheme of the triggering setup

Special care was paid on the synchronisation of the bubble generation, plasma ignition and ICCD imaging. A laser beam, very close to the tip of the capillary, propagating through the liquid was detected with a phototransistor (Fig. 1 (a)). When a gas bubble intercepts the laser pathway, the phototransistor signal turns to zero due to light deviation at the liquid-gas interfaces (Fig. 1 (b)). The phototransistor switch was used as a trigger for the control of both the PG power supply and the ICCD gating. This technique showed a reproducible behaviour of the phototransistor on/off signal for the gas flow rate used in this work. The pulse train (red lines in Fig. 2) duration was controlled to study different liquid treatment conditions. In Fig. 2 , we illustrate a plasma ignition: the plasma is continuously produced even between bubbles, we call this the continuous mode (Fig. 2 (1)), the whole life-time of the bubble (Fig. 2 (2)) and the first-half (Fig. 2 (3)). In our experiment, we also initiate the plasma during a quarter, an eighth of time of the bubble at different moment of the bubble expansion. For the case of 12 sccm, the bubbles are detected during about 350 ± 40 ms and time

between bubbles is 100 ± 30 ms. The jitter is probably due to slight variations of the bubble dynamic that might affect the laser spot movement.

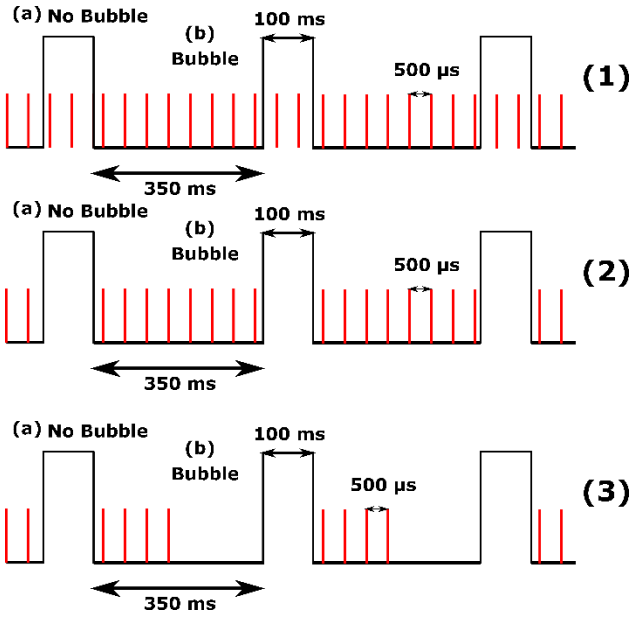

Fig. 2 Illustrations of the triggered signals; Pulse train during in (1) the continuous mode, (2) the whole time of the bubble, (3) the first-half time of the bubble.

To record the plasma emission during the full duration of one voltage pulse and reduce the stray light from the experimental room and the laser beam, a typical 20 µs ICCD gating was selected. Light reflections from the PG capillary were prevented by covering this one with a black dielectric cover.

3. Results and discussion

3.1. Plasma generation in bubbles

Fig. 3 presents images of the plasma in bubbles at the beginning of the treatment (0) and after 10 and 20 min at different times of evolution of the bubble in distilled water. At the very beginning of the treatment (0 min in Fig. 3) in distilled water (low conductivity: ~5 µS/cm), the plasma expansion from the PG capillary occurs in the whole volume of the bubble and exhibits a rather diffuse pattern, even when the bubble reaches its maximum volume. After 10 min and 20 min of treatment, the conductivity has increased and reached respectively 70 µS/cm and 135 µS/cm. In those cases, the plasma does not propagate in the whole bubble. It reaches ~ 1.4 mm maximum after the outlet capillary which is two times less than at the beginning of the treatment. Moreover, it has a non-diffuse pattern with well localized filaments on the bubble boundaries. The Fig. 3 clearly shows the influence of the water conductivity on the plasma propagation and shape inside the bubble.

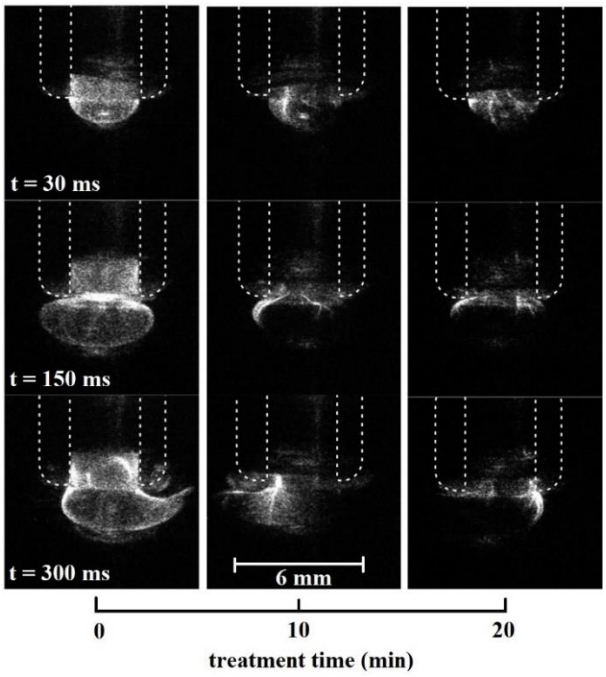

Fig. 3 Images of the plasma for different time treatment: 0, 10 and 20 min in distilled water. Exposure time: 20 µs.

To confirm the role of the conductivity on plasma propagation, we imaged the plasma inside bubbles produced in tap water which is more conductive than distilled water. The Fig. 4 shows at a delay of 100 ms after the bubble generation the plasma expansion in distilled water (on the right) and tap water (on the left). In the tap water, of higher conductivity (~340 µS/cm), the plasma seems filamentary and propagates less than 1 mm in the bubble. The key role of the dielectric or conductive nature of the liquid at the boundaries of the gas bubble is evidenced and correlates with previously reported propagation of plasma over dielectric or conductive but solid targets [6]. It was reported that with conductive target the plasma plume connects on a small size spot while plasma can expands over dielectric targets covered with a rare gas (helium or neon) layer.

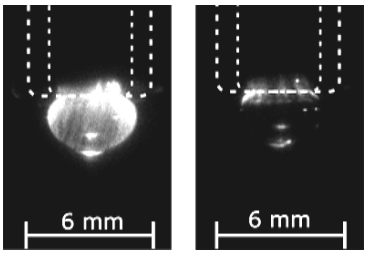

Fig. 4 Plasma emission in neon-bubble generated at 2 kHz with 12 sccm flow rate in distilled water (left) and in tap water (right). Exposure time: 20 µs.

3.2. Conductivity measurements in distilled water

Fig. 5 presents the conductivity measurements for two conditions of treatment. One with the capillary immersed 1cm in the liquid and one 3mm above the liquid. For both cases, the evaporation is 0.2 ml and the temperature went from 20°C to 26°C after 20min of treatment. We checked there was no effect on conductivity measurements. For the treatment in the liquid, after 10 min, the conductivity increases faster than above the liquid. When the capillary is above the liquid, the plasma interacts with the surrounding air, inducing a different chemistry compared to the immersed case.

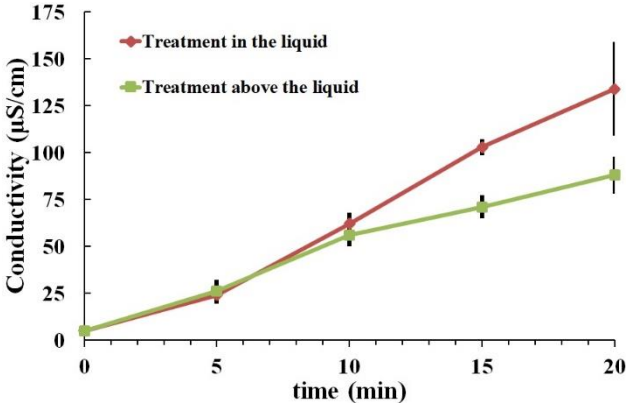

Fig. 5 Time evolution of the conductivity in distilled water

3.3. Influence of plasma on bubble growth

The bubble growth dynamics was assessed from time resolved ICCD images by reporting the evolution of the on-axis bubble height from the capillary outlet versus time. In the very first instants the bubble is not detected. When it is detected, the bubble has already reached 1 mm and the treatment start. Fig. 6 presents the on-axis bubble height time of evolution for 12 sccm gas flow rate without plasma (Fig. 6 red curve) and for three train pulse conditions. One during the first 175 ms of the bubble growth (Fig. 6 green curve), and the second starting from 175 ms to 350 ms (Fig. 6 purple curve). As previously shown in [7], when the plasma is initiated at the beginning of the bubble grow, the bubble height rapidly increases during the first 50 ms and then stabilizes around 4 mm until around 300 ms delay from bubble emergence. For the same neon flow rate but with no plasma ignition, the bubble expansion is drastically slower and does not reach the same 4 mm excursion from capillary tip during the 300 ms time window. At the beginning, the initiation of the plasma during the first half of the bubble evolution follows the same pattern than full time treatment. Then, at 175 ms (Fig. 6 green curve) when the plasma is off, the bubble front move forward. Finally, it growth again and almost reach the maximum bubble front propagation at 4 mm. Conversely, the plasma initiation at 175 ms of the bubble growth (Fig. 6 purple curve) exhibits a similar behaviour than when the plasma is off (Fig. 6 red curve). The case of continuous plasma initiation was not depicted here but gives identical feature than the Plasma is off (Fig. 6 red curve). These measurements show that plasma ignition has a key influence on bubble growth. The action being partly associated with a gas flow rate modification but also probably associated with pressure burst or small gas heating and consecutive neon density modulation following plasma ignition. We also probably have the channelling action of plasma recently confirmed for helium, neon or argon feeding gas [8].

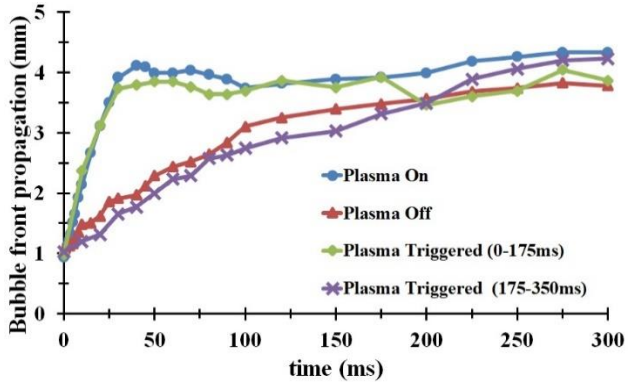

Fig. 6 Evolution of the bubble growth at 12 sccm neon flow rate with and without plasma and at different initiation conditions

3.5. Production of hydrogen peroxide, nitrates and nitrites.

Table 1 presents the average concentration per discharge of hydrogen peroxide, nitrates and nitrites create with different plasma treatment. The first column in Table 1 presents the results for a treatment above the liquid, the others are for different treatments in the liquid. The pulse train during the half, the quarter and the eighth of time of the bubble were performed at different time of the bubble expansion.

Table 1 . Average concentration per discharge of hydrogen peroxide, nitrates and nitrites for 20 min of treatment of distilled water

	Above the liquid	Continuous mode	Full time	Half time	Quarter time	Eighth time
Bubble time (ms)	-	-	341	350	365	345
Plasma time (ms)	-	-	341	175	91	43
H_2O_2 [mg/L]/ discharge	4,2E-06	1,3E-05	1,7E-05	9,5E-06	1,9E-05	2,3E-05
NO_3^- [mg/L]/discharge	4,2E-05	1,1E-05	1,4E-05	9,5E-06	1,9E-05	3,9E-05
NO_2^- [mg/L]/discharge	4,2E-07	4,2E-07	5,5E-07	9,5E-07	1,9E-06	3,9E-06

According to these measurements, when we initiate the plasma during the quarter or the eight of time of the bubble, the treatment is more efficient than full or half-time mode. Moreover, the application of the same pulse train during different times of the bubble expansion exhibits the same

efficiency. In continuous mode, the efficiency is lower than the full-time mode, while the final concentration after 20 min is the same. Finally, above the liquid, the treatment produces more nitrates and less hydrogen peroxide per discharge than inside the liquid.

These results show that the chemistry inside the capillary, when there is no bubble, is almost negligible for the distilled water treatment. The species creation efficiency does not depend on the timing of the application of pulse train. Indeed, if we treat an eighth of time for the first 45 ms or between 130 and 175 ms (Fig. 6 blue curve) we obtain the same efficacy. Since the volume of the bubble evolves, we can say that the efficacy of the treatment does not depend on the volume. This indicates that the induced chemistry inside the bubble leads to a kind of global equilibrium between species. The creation of hydrogen peroxide is more important when the treatment is done under the surface and was reported in [4]. For the nitrate, it is higher when the treatment is done on the surface. This higher efficiency for the nitrate formation is due to the mixing between the air and neon flow. Conversely, in the bubble, we only have a mixing with the water vapor and not enough nitrogen to create the same amount of nitrate.

4. Conclusion

The generation of plasma in bubbles emerging from the plasma gun capillary flushed with very small gas flow rate of neon and immersed into liquid solution has been demonstrated and characterized by ICCD imaging. The key role of water solution conductivity results in different plasma expansion in gas bubble. Plasma expansion in bubble appears to be much stronger at the gas-liquid interface. It is much more filamentary when liquid solution is highly conductive. The strong influence of plasma generation on bubble growth dynamics has also been documented. It is suggested that plasma has partly action on the gas flow features at the capillary outlet but also probably induces pressure modulation of gas inside bubbles in comparison with bubble generated with no plasma ignition. More work is in progress to analyse these phenomena. It would be important to consider developing plasma chemistry models in plasma in bubble surrounded by a liquid. This would be interesting to run simulation for long treatment times, above or inside the liquid, also for different plasma treatments.

These different ways to initiate the plasma should be considered when trying to analyse plasma activated liquids properties obtained in different solutions or for different treatment duration. With our setup, treatment of distilled water solutions over few minutes is associated with a drastic evolution of the liquid conductivity. Then, it drives a modification in the plasma generation in bubble during the plasma delivery. Concentration measurements show that the creation of species is not directly related to the volume of the bubble. It is also better to shorten the plasma treatment to have a better efficiency. In our conditions, we can think about the possibility to use multi-bubble system to treat greater volumes of water with a better efficiency for the creation of reactive species.

Acknowledgments

AH is supported by MENSR PhD fellowship.

References

[1] P J Bruggeman et al 2016 Plasma Sources Sci. Technol. **25** 053002

[2] Wei Tian et al 2014 J. Phys. D: Appl. Phys. **47** 055202

[3] Kunihide Tachibana et al 2011 Plasma Sources Sci. Technol. **20** 034005.

[4] Xiujuan J. Dai et al 2016 Plasma Process. Polym, **13** 306-310

[5] Eric Robert et al 2009 Plasma Process. Polym, **6** 795-802

[6] Eric Robert et al 2014 Plasma Sources Sci. Technol. **23** 12003

[7] Audoin Hamon et al 2018 Int. Conference on Gas Discharges and Their Applications (Novi Sad, Serbia September 2018)

[8] Xavier Damany et al 2017 Int. Workshop. on Microplasmas (Garmisch–Partenkirchen, Germany June 2017)